

Figure S2. Flow cytometric analysis of retrotransposition-positive HC11 cl.11 cells. Control HC11 or HC11 cl.11 cells were analyzed by using flow cytometry for EGFP expression. Dot plots are presented for each sample. UL and UR contain retrotransposition-negative and retrotransposition-positive cells, respectively; 11.48% value in HC11 cl.11 data represents the net retrotransposition frequency, subtracted by a 0.44% of false-positive cells.

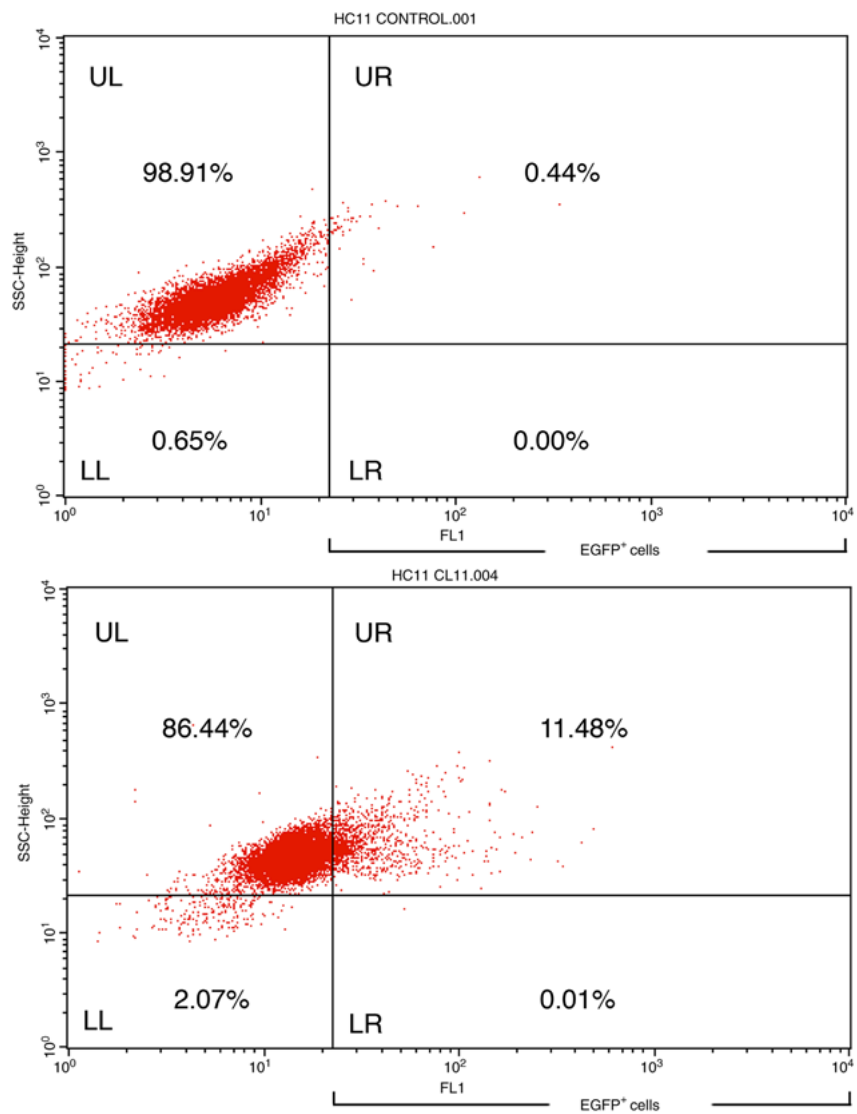


Figure S3. Induced epithelial-mesenchymal transition and multinucleation in VL30 retrotransposition-positive HC11 cells. (A) Normal HC11 and (B) retrotransposition-positive HC11 cl.11 cells in normal culture dishes; magnification, x20. HC11 cl.11 cells cultured on glass coverslips were fixed with 3.7% paraformaldehyde and images were captured under normal (C) or UV light (D); magnification, x40. White arrow (C) indicates a large multinucleated cell overlaid with EGFP retrotransposition-positive cells (D).

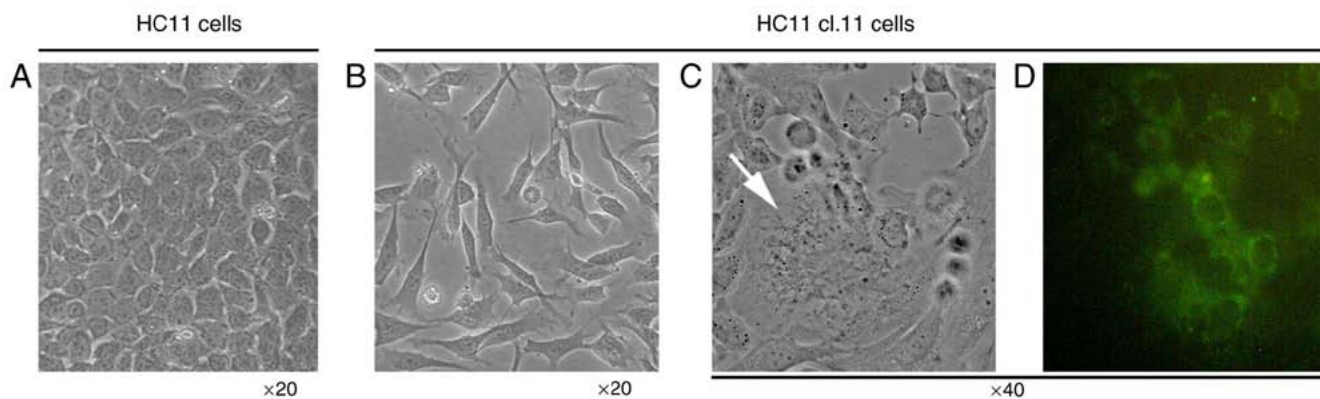


Figure S4. Tinzaparin inhibits serum starved- and VEGF-induced VL30 retrotransposition of mouse NIH3T3 fibroblast cells. Pcl.10 cells, harboring the recombinant plasmid NVL-3*/EGFP-INT, were treated as indicated. Results are presented as the mean \pm SD of duplicate samples from three independent experiments. **P<0.01 and ***P<0.001 (one-way ANOVA followed by Tukey's test).

